

## Hexameric subphthalocyanine rosette†

Mitsuhiko Morisue,\* Wataru Suzuki and Yasuhisa Kuroda

Received 27th June 2011, Accepted 26th July 2011

DOI: 10.1039/c1dt11214g

A highly congested hexameric subphthalocyanine array was synthesized by axial chlorine-to-phenoxy substitution of a hexakis(4-hydroxyphenyl)benzene based subphthalocyanine, and photoinduced symmetry-breaking charge separation was demonstrated in polar solvent.

## 1. Introduction

The bacterial light-harvesting antenna complex (LH2) forms a wheel structure to funnel light-energy over a relatively long range during the primary photosynthetic event.<sup>1</sup> Cyclic arrays of 18 $\pi$ -electron macrocycles, such as porphyrins and phthalocyanines, have been the subject of considerable synthetic effort to produce models of the LH2 complex and gain insight into the fundamental process of the primary photosynthesis.<sup>2–5</sup> A template-directed synthetic methodology can provide a precise synthetic route to chromophore arrays controlled by an appropriate template molecule.<sup>3–5</sup> Hexa-substituted benzene is a versatile scaffold for forming six-fold symmetric chromophore arrays as successful models of the LH2 system. At the same time, hexaphenylbenzene derivatives are intriguing due to possible gear rotation around the radial bonds—the so-called “molecular rotors”.<sup>6</sup> Thus, photodynamics might be tunable due to rotational motions in the six-fold LH2 model. The present study has designed radial subphthalocyanine (SubPc) arrays using a hexaphenylbenzene derivative as a scaffold for six 14 $\pi$ -electron macrocycles.

SubPc is a ring-contracted homologue of phthalocyanine and is a curvature of 14 $\pi$ -electron macrocycle.<sup>7</sup> The facile exchange of axial chlorine to a phenoxy group has been previously employed to introduce functional groups to SubPc.<sup>8–9</sup> However, this reaction has not been applied to the synthesis of multichromophore arrays with more than three SubPc units.<sup>10</sup> Here we disclose the synthesis and photophysical properties of a systematic series of SubPc arrays (Scheme 1).

## 2. Results and discussion

## 2.1. Synthesis and structural characterization

Reflux of hexakis(4-hydroxyphenyl)benzene with excess Cl[B(SubPc)] in toluene gave *hexa*-[B(SubPc)] **1** in 46% isolated yield despite requiring multiple reactions at highly congested sites. The SubPc derivatives were identified using

NMR (Fig. 1). MALDI-TOF MS showed the parent peak and partial fragmentation peaks, and analytical size-exclusion chromatography showed only the unimodal peak, indicating that the phenoxy sites were completely substituted with SubPc (Fig. 2). Full accommodation of the multiple hydroxyl sites was successful in all members of the systematic series of *hexa*-[B(SubPc)] **1**.

The  $\beta$ -phenyl protons of the axial phenoxy group showed a gradual shift upfield due to shielding by the SubPc macrocycle as the number of SubPc subunits is increased (Fig. 1). On the other hand, the upfield shift (relative to PhO[B(SubPc)] **4**) of the  $\alpha$ -phenyl protons of *hexa*-[B(SubPc)] **1** is smaller than the shifts for *mono*-[B(SubPc)] **3** and *bis*-[B(SubPc)] **2**, suggesting deshielding by the lateral edge of the SubPc macrocycle attached to the neighbouring phenoxy branch. Thus, the hook-shaped axial Ph–O–B bond at the centre of the SubPc macrocycle penetrates into the “bay” region of the neighboring SubPc to mitigate possible intramolecular steric congestion (Fig. 2). Such a configuration may restrict internal rotation of the SubPc subunits.

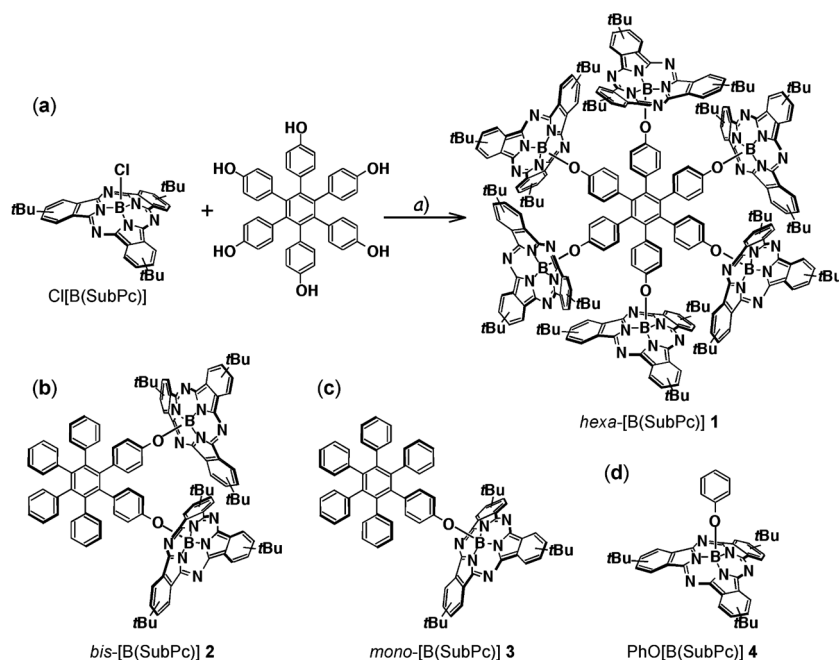
Mutual ring currents within the SubPc subunits divide the signals from the SubPc subunits into shielded and unshielded protons, as assigned by <sup>1</sup>H–<sup>13</sup>C HMQC NMR.<sup>11</sup> Each of the  $\alpha_{(4)}$  and  $\beta$ -protons of *hexa*-[B(SubPc)] **1** is split into two sets of signals: one set of  $\alpha_{(4)}$  and  $\beta$  protons at 7.85 and 8.55 ppm with no significant shift and the other at 7.75 and 8.3 ppm with large upfield shift, respectively. The  $\alpha_{(1)}$  protons were split to 8.6 and 8.8 ppm in the similar way. Interestingly, no cross-peak was observed for these two sets of split signals in <sup>1</sup>H–<sup>1</sup>H TOCSY NMR spectrum (Fig. 3), suggesting that the internal rotation of the SubPc subunits is prevented. On the other hand, rotational motions were not restricted in *bis*-[B(SubPc)] **2** and *mono*-[B(SubPc)] **3**. Therefore, the cyclic array of hexameric bulky SubPc macrocycles apparently enforces spiral interdigitation of SubPc subunits, leading to interlocking of their internal rotations.

## 2.2. Photophysical properties

Both the absorption and fluorescence maxima of the degenerate Q band show only a marginal change for *bis*-[B(SubPc)] **2** and *hexa*-[B(SubPc)] **1** compared to PhO[B(SubPc)] **4** or *mono*-[B(SubPc)] **3** (Fig. 4a and 4c). However, the intensity of the Q band of *hexa*-[B(SubPc)] **1** is much smaller than a summation of the

Department of Biomolecular Engineering, Kyoto Institute of Technology, Matsugasaki, Sakyo-ku, Kyoto, 606-8585, Japan. E-mail: morisue@kit.ac.jp

† Electronic supplementary information (ESI) available. See DOI: 10.1039/c1dt11214g



**Scheme 1** Synthesis of *hexa*-[B(SubPc)] **1**; a) reflux in dry toluene, 46% (a). Chemical structures of *bis*-[B(SubPc)] **2** (b), *mono*-[B(SubPc)] **3** (c), and PhO[B(SubPc)] **4** (d).

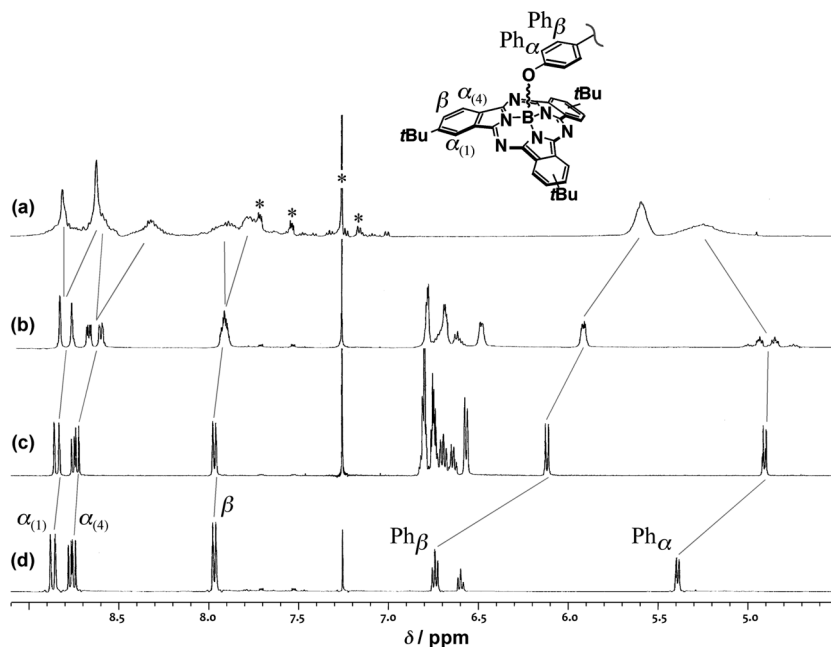


**Fig. 1**  $^1\text{H}$  NMR spectra (500 MHz, in  $\text{CDCl}_3$ ) of *hexa*-[B(SubPc)] **1** (a), *bis*-[B(SubPc)] **2** (b), *mono*-[B(SubPc)] **3** (c), and PhO[B(SubPc)] **4** (d) at 25 °C. Asterisk indicates residual solvent and impurity.

contributions from the six SubPc subunits would predict: the molar extinction of a SubPc subunit in *hexa*-[B(SubPc)] **1** is approximately half-magnitude of that of the SubPc unit of *mono*-[B(SubPc)] **3** (Fig. 4b). In principle, hypochromism originates from dispersion force interactions between transition dipoles, as exemplified by polynucleotides.<sup>12</sup> The reduced oscillator strength minimizes exciton coupling among the SubPc subunits; therefore, the degenerated Q band is observed even in the highly congested *hexa*-[B(SubPc)] **1**.

Fast energy migration through multichromophore arrays redistributes the polarization of excited states.<sup>3</sup> Stationary fluorescence anisotropy experiments, using polyethylene glycol ( $M_w = 200$ ) as viscous medium, revealed the occurrence of energy migration between the SubPc subunits (Fig. 5). Intrinsic redistribution of the fluorescence of PhO[B(SubPc)] **4** is relatively significant because of the degenerated Q band (Fig. 5a and 5e), while that for *mono*-[B(SubPc)] **3** is reduced by introduction of the bulky hexaphenylbenzene due to slower rotational diffusion (Fig. 5b

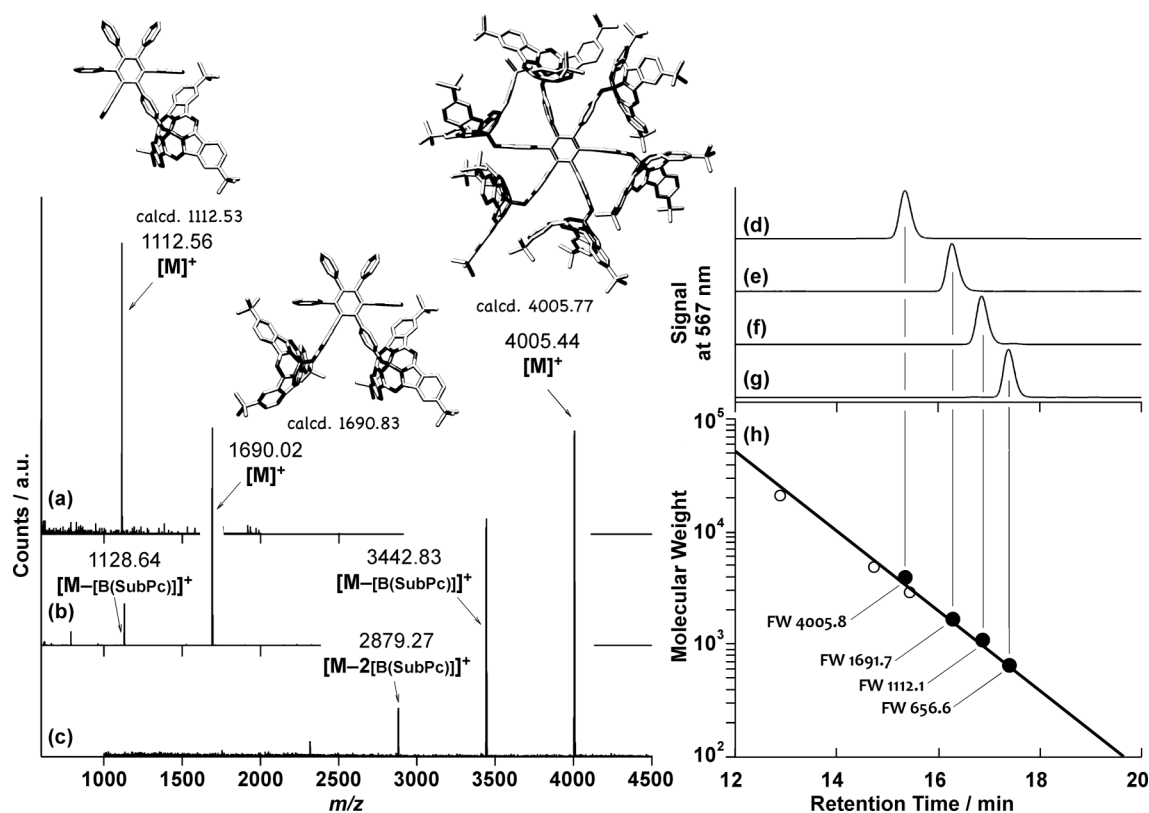


**Fig. 2** MALDI-TOF MS spectra and analytical size-exclusion chromatogram of *mono*-[B(SubPc)] **3** (a and f), *bis*-[B(SubPc)] **2** (b and e), *hexa*-[B(SubPc)] **1** (c and d), and PhO[B(SubPc)] **4** (g), and a logarithmic plot of their molecular weight against retention time (filled circles) referenced against polystyrene as a standard (open circles) (d). Geometry-optimized structures, produced using the HyperChem package, are depicted having  $C_3$ -symmetry though they are produced as isomeric mixtures, the hydrogen atoms are omitted for visual clarity.

**Table 1** Fluorescence lifetime  $\tau_F$  in toluene and DMSO<sup>a</sup>

	$\tau_F$ in toluene	$\tau_F$ in DMSO
PhO[B(SubPc)] <b>4</b>	1.9 ns	1.7 ns
<i>mono</i> -[B(SubPc)] <b>3</b>	1.9 ns	1.7 ns
<i>bis</i> -[B(SubPc)] <b>2</b>	1.9 ns	124 ps, 1.1 ns, 1.8 ns
<i>hexa</i> -[B(SubPc)] <b>1</b>	1.9 ns	73ps, 827 ps, 3.4 ns

<sup>a</sup> Observed using a 200-fs laser pulse at 488 nm.

and 5f). Redistribution of the fluorescence polarization in *hexa*-[B(SubPc)] **1** is much greater than that in *mono*-[B(SubPc)] **3** and *bis*-[B(SubPc)] **2** despite it being of larger molecular size.

Energy migration is also suggested by time-resolved fluorescence measurements, which do not show a dependence on excitation power when using a 200 fs laser pulse (50–180  $\mu$ W, excitation at 488 nm). Possible annihilation of the excited singlet excitons may occur by energy migration on a time scale shorter than the time resolution of the present experimental conditions.

All the SubPc derivatives exhibited identical single component decay profiles with fluorescence lifetimes of 1.9 ns in the nonpolar solvent toluene (Table 1 and Fig. 6). Therefore, the locally excited singlet hops among the SubPc subunits prior to monomeric emission, irrespective of the number of SubPc subunits.

It was noticeable that the fluorescence quantum yields ( $\Phi_F$ ) of *bis*-[B(SubPc)] **2** and *hexa*-[B(SubPc)] **1** showed a steep

decline with increased solvent polarity (Fig. 4d), while neither hypsochromic/bathochromic shift nor excimer fluorescence was observed regardless the number of the SubPc subunits. Excited state decay profiles of *hexa*-[B(SubPc)] **1** and *bis*-[B(SubPc)] **2** in DMSO indicated three components processes.<sup>11</sup> In contrast, monomeric SubPc **3** and **4** retained similar  $\Phi_F$  values and fluorescence lifetimes of 1.7 ns in polar DMSO as a polar solvent (Fig. 4d and Table 1). Small Stokes shift of SubPc was not susceptible to the solvent polarity in a wide range of orientation polarizability of the solvent ( $\Delta f$ );

$$\Delta f = f(\epsilon_r) - (n_D^2 - 1)/(2n_D^2 + 1)$$

wherein  $f(\epsilon_r)$  is the solvent polarity parameter as defined by  $f(\epsilon_r) = (\epsilon_r - 1)/(2\epsilon_r + 1)$ ,  $\epsilon_r$  is the relative dielectric constant, and  $n_D$  is the refractive index.<sup>11</sup> In accordance with the Lippert–Mataga principle, this observation suggests that there is little change in the inherent polarization of the SubPc chromophore upon photoexcitation.<sup>11,13</sup> The contrasting result implies that the solvent susceptibility of the fluorescence of SubPc derivatives originates from interchromophore interactions.

The present evaluation employs  $f(\epsilon_r)$  as the index according to Mataga's analytical procedures for similar solvation-induced polarization phenomena for 1,2-di(9-anthryl)ethane and 9,9'-bianthryl.<sup>14a</sup> The plot of  $\Phi_F$  values for *hexa*-[B(SubPc)] **1** and *bis*-[B(SubPc)] **2** drops off suddenly, when the solvent polarity parameter,  $f(\epsilon_r)$ , is larger than 0.45 (Fig. 4d), which closely mirrors Mataga's observations.<sup>14a,15</sup>

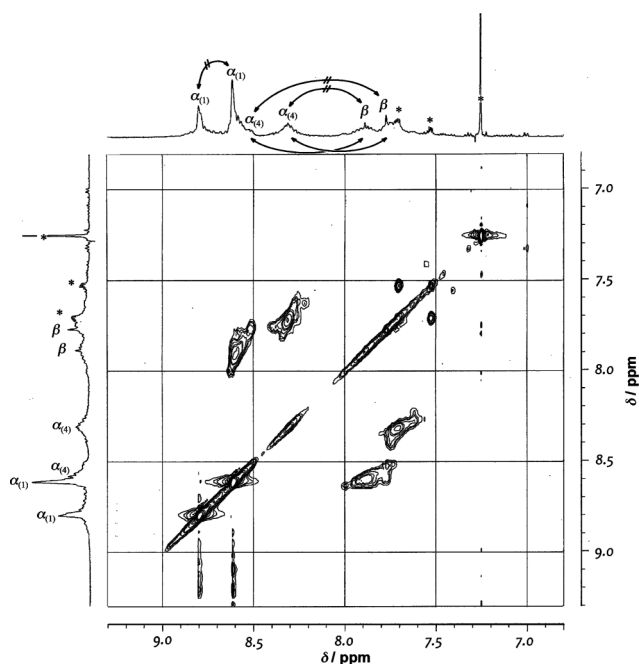


**Fig. 3** Representative  $^1\text{H}$ - $^1\text{H}$  TOCSY NMR spectrum of *hexa*-[B(SubPc)] **1** in  $\text{CDCl}_3$  at  $25^\circ\text{C}$ . Arrows indicate the correlation among the signals, and arrows with interception denotes no correlation among the corresponding signals. Asterisk indicates residual solvent and impurity.

The solvent dependence strongly suggests the formation of a non-fluorescent excimer in polar solvents, *i.e.*, photoinduced

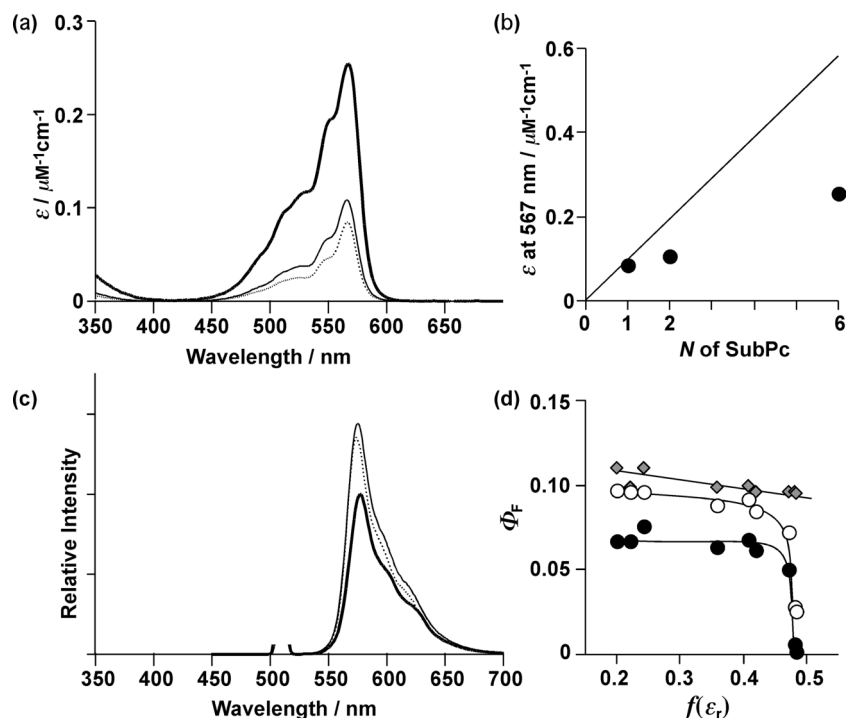


**Fig. 4** Absorption (a) and fluorescence spectra (c) of *hexa*-[B(SubPc)] **1** (thick line), *bis*-[B(SubPc)] **2** (solid line), and *mono*-[B(SubPc)] **3** (dotted line) in toluene at  $25^\circ\text{C}$ . Plot of the extinction coefficient at  $567\text{ nm}$  versus number of SubPc subunit (filled circle) and the proportional relation (solid line) based on the value of PhO[B(SubPc)] **4** (b). The fluorescence spectra are normalized to the corresponding absorbance at  $510\text{ nm}$  of the excitation wavelength. Plot of the fluorescence quantum yield of *hexa*-[B(SubPc)] **1** (filled circle), *bis*-[B(SubPc)] **2** (open circle), *mono*-[B(SubPc)] **3** (filled square) and PhO[B(SubPc)] **4** (grey square) in aprotic solvent as a function of the solvent polarity parameter,  $f(\epsilon_r)$  (d).

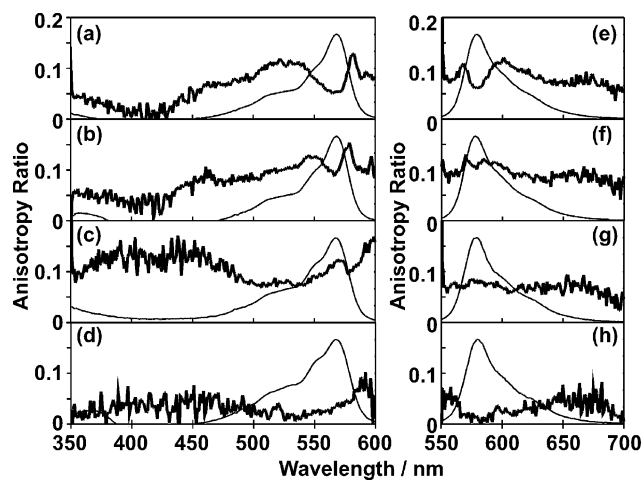


**Fig. 5** Steady-state excitation anisotropy spectra (thick line, a–d) monitored at  $610\text{ nm}$  and normalized absorption spectra (thin line, a–d), and fluorescence anisotropy spectra (thick line, e–h) and normalized fluorescence spectra (thin line, e–h) excited at  $510\text{ nm}$  of PhO[B(SubPc)] **4** (a and e), *mono*-[B(SubPc)] **3** (b and f), *bis*-[B(SubPc)] **2** (c and g), and *hexa*-[B(SubPc)] **1** (d and h) in PEG. The maximum wvelengths of the non-polarized excitation spectra were identical with those of the corresponding absorption.

symmetry-breaking charge separation of identical multichromophore systems. This phenomenon has been observed for a few multichromophore systems, in which their electronic coupling is usually weak.<sup>16–18</sup> The structure of the series of *hexa*-[B(SubPc)] **1**

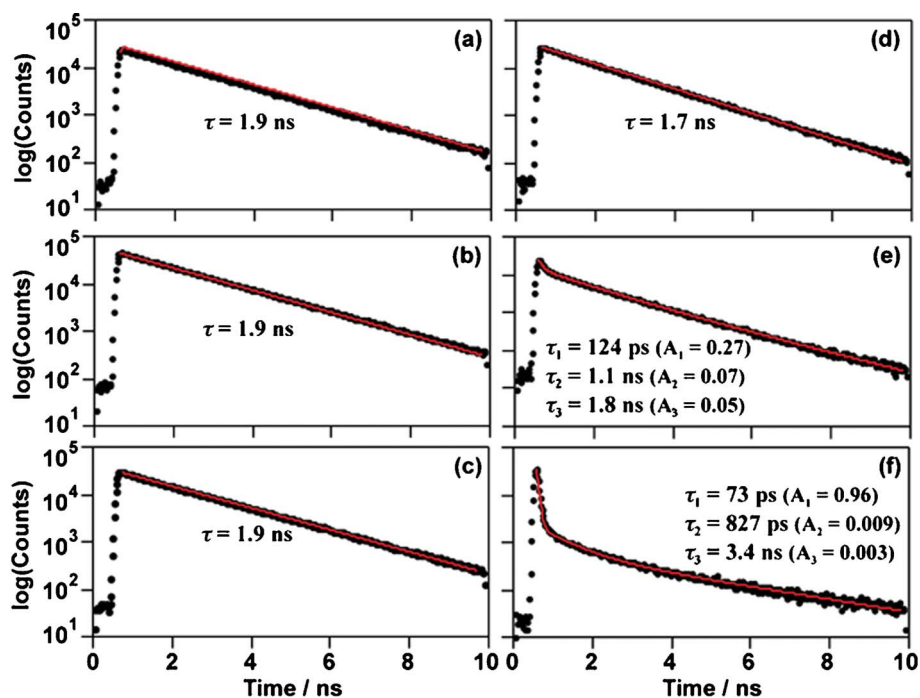
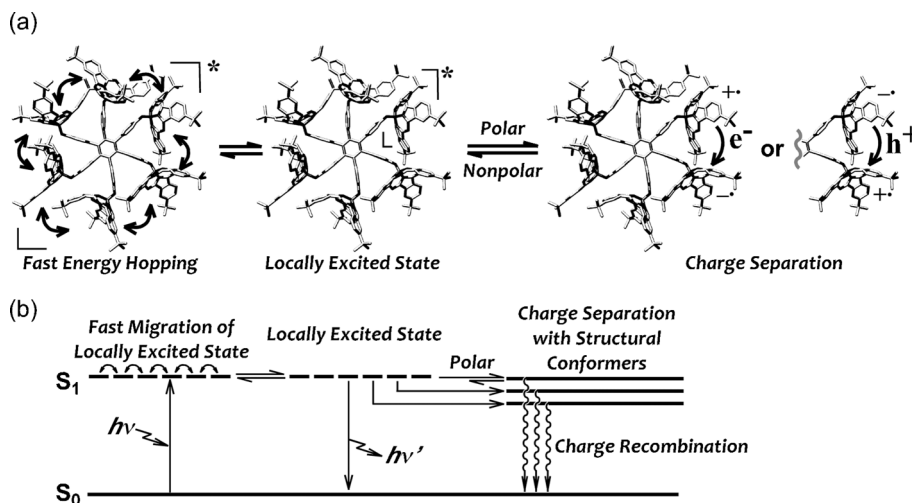


**Fig. 6** Fluorescence decay kinetics of *mono*-[B(SubPc)] **3** in toluene (a) and in DMSO (d), *bis*-[B(SubPc)] **2** in toluene (b) and in DMSO (e), and *hexa*-[B(SubPc)] **1** in toluene (c) and in DMSO (f). Red line indicates the regression analysis with time constant(s) as summarized in Table 1.



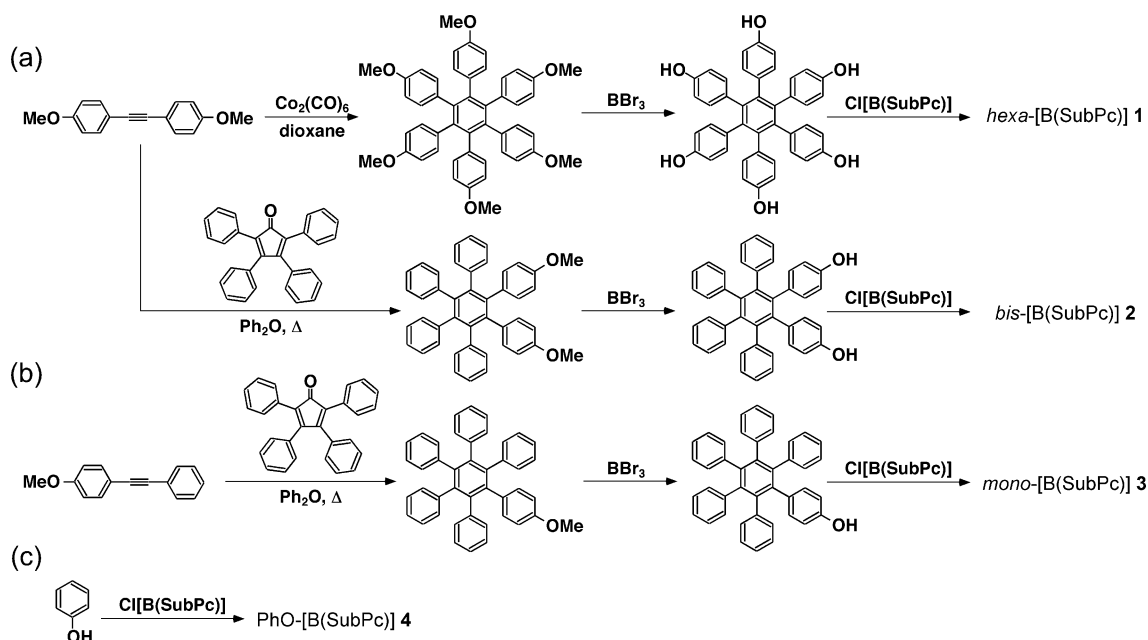
**Scheme 2** Schematic representation of plausible photophysical processes of *hexa*-[B(SubPc)] **1** (a) and its Jablonski diagram (b).

is likely to fulfill the geometrical prerequisite for the symmetry-breaking charge separation. To our best knowledge, the present observation is the first finding of the symmetry-breaking charge separation for SubPc. Several reports suggest that charge separation undergoes an equilibrium between a locally excited (neutral) state and a zwitterionic (charge transfer) state.<sup>16b,d</sup> The fluorescence lifetimes of 3.4 ns observed for *hexa*-[B(SubPc)] **1** longer than the normal fluorescence decay imply a re-excitation path through such equilibrium. Solvent fluctuations lead to structural relaxation in a dissymmetric fashion, which induces charge transfer in a random direction; namely symmetry-breaking in the identical chromophores. Therefore SubPc subunits reorient are predicted to stabilize the geminated ion pair.<sup>14</sup>

Scheme 2 illustrates the possible photophysical processes. When SubPc is photoexcited, the excited singlet migrates on the SubPc arrays. If the solvent medium is nonpolar, the locally excited state shows monomeric emission. On the other hand, the polar solvent induces the symmetry-breaking charge separation. The multi-exponential decay profiles observed in the present experiments can be explained by the existence of structural conformers.

### 3. Summary

In summary, a synthetic model of the LH2 complex incorporating SubPc has been successfully accomplished by axial chlorin-to-phenoxy substitution using a hexaphenylbenzene derivative as the scaffold. The systematic series of SubPc arrays give insight



**Scheme 3** Synthetic routes of *hexa*-[B(SubPc)] **1** and *bis*-[B(SubPc)] **2** (a), *mono*-[B(SubPc)] **3** (b), and PhO[B(SubPc)] **4** (d).

into highly congested SubPc architecture with particular focus on their structural and photophysical features. Internal motion of *hexa*-[B(SubPc)] **1** was restricted under ambient conditions. Such dynamic motion was controlled by the solvent polarity as observed through photoinduced symmetry-breaking charge separation. Further elucidation of structural and photophysical dynamics is currently being undertaken in our group.

## 4. Experimental

### 4.1 General method

$^1\text{H}$ ,  $^{13}\text{C}$ , and 2D NMR spectra were recorded on spectrometers (ARX 500 or AVANCE 300, BRUKER) using TMS as the internal standard in  $\text{CDCl}_3$ . MALDI TOF-MS spectrometry was observed with dithranol as a matrix by BRUKER AUTOFLEX II. Analytical size-exclusion chromatogram was performed by a LC-NetIII/ADC (JASCO) equipped with columns of Shodex KF-802.5 and KF-804 L (Showa Denko Co.) with  $\text{CHCl}_3$  as the eluent. UV-visible and fluorescence spectra were recorded on the spectrophotometer (Multispec-1500, Shimadzu) and the fluorescence photospectrometer (F-4500, Hitachi), respectively. The fluorescence quantum yield was determined by comparing with the fluorescence of Cl[B(SubPc)] in benzene ( $\Phi_{\text{F}} = 0.16$ ).<sup>15</sup> Time-resolved fluorescence measurements were carried out by employing a circularly polarized beam from a continuous wave (CW)  $\text{Ar}^+$  laser (LGK7872M, LASOS) with an excitation wavelength of 488 nm and a streak camera to detect the fluorescence.

### 4.2 Synthetic procedures

A silica-gel column (Wakogel C-200, Wako Chemical Co.) and a Sephadex column (LH-20, GE Healthcare Co.) were used for chromatographic purification. All solvents were dried prior to use.

The phenol precursors with a hexaphenylbenzene framework were prepared by diverse approaches (Scheme 3). 1,2-

Bis(4-hydroxyphenyl)-3,4,5,6-tetrakis(phenyl)benzene was prepared by Diels–Alder cycloaddition of 2,3,4,5-tetraphenyl-2,4-cyclopentadien-1-one and 4-bis(4-methoxyphenyl)acetylene, followed by removal of the methyl groups by boron tribromide, using a synthetic procedure similar to that reported for 1-(4-hydroxyphenyl)-2,3,4,5,6-pentakis(phenyl)benzene<sup>19</sup> On the other hand, hexakis(4-hydroxyphenyl)benzene was synthesized by demethylation of hexakis(4-methoxyphenyl)benzene, which was prepared by  $\text{Co}_2(\text{CO})_8$ -catalyzed cyclotrimerization of bis(4-methoxyphenyl)acetylene, according to literature procedures.<sup>20</sup> It should be noted that it is difficult to compare the isolated yields of the SubPc derivatives **1–4** because of the differences in the reaction conditions necessitated by the solubility of the precursor hexakis(phenyl)benzene derivatives in toluene.

### 4.3. Hexakis{4-[2,9(10),16(17)-tris(*tert*-butyl)subphthalocyaninato]oxyphenyl}benzene, *hexa*-[B(SubPc)] **1**

A mixture of hexakis(4-hydroxyphenyl)benzene<sup>20</sup> (14 mg, 0.023 mmol) and Cl[B(SubPc)] (83 mg, 138 mmol) was refluxed in dry toluene (4 mL) for 24 h. The reaction mixture was refluxed with additional Cl[B(SubPc)] (50 mg, 83 mmol) for an additional 48 h. The mixture was washed with saturated aqueous sodium hydrogencarbonate (20 mL) and brine (20 mL). The residue was purified by silica-gel column chromatography with *n*-hexane/ethyl acetate (gradient from 5/1 to 4/1, v/v) as the eluent, followed by a Sephadex column with ethyl acetate. The desired material was obtained as a purple solid (42 mg, 11  $\mu\text{mol}$ ; yield 46% based on hexakis(4-hydroxyphenyl)benzene).  $^1\text{H}$  NMR (300 MHz,  $\text{CDCl}_3$ ):  $\delta = 8.68$ – $8.47$ ,  $8.93$ – $8.68$  (brm, 18H; SubPc- $\alpha_{(1)}$ ),  $8.07$ – $7.67$  (brm, 18H; SubPc- $\beta$ ),  $5.73$ – $5.48$  (brm, 12H; Ph  $\beta$  to O-B(SubPc)),  $5.48$ – $4.95$  (brm, 12H; Ph  $\alpha$  to O-B(SubPc)),  $8.47$ – $8.14$ ,  $8.77$ – $8.68$  (brm, 18H; SubPc- $\alpha_{(4)}$ ),  $1.60$ – $1.37$  ppm (brm, 162H; *t*Bu).  $^{13}\text{C}$  NMR (125 MHz,  $\text{CDCl}_3$ ):  $\delta = 153.5$ – $153.2$  (br),  $151.3$ – $150.6$  (br),  $149.3$ – $149.5$  (br),  $139.2$ ,  $134.2$ ,  $131.5$ – $131.0$  (br),  $128.8$ – $128.5$  (br),  $127.6$ ,

122.3–121.7 (br), 119.2–118.8 (br), 118.5–117.8 (br), 35.8–35.6 (br), 31.7 ppm. MALDI-TOF MS:  $m/z$  calcd for  $C_{258}H_{240}B_6N_{36}O_6$  4005.77; found 4005.44  $[M]^+$ . UV-vis (toluene):  $\lambda_{\max}$  = 567 nm (Q band).

#### 4.4. 1,2-Bis(4-hydroxyphenyl)-3,4,5,6-tetraphenylbenzene

2,3,4,5-Tetraphenyl-2,4-cyclopentadien-1-one (275 mg, 0.72 mmol) was refluxed with 1,2-bis(4-methoxyphenyl)acetylene (170 mg, 0.71 mmol) in diphenylether (2 mL) for 12 h. The reaction mixture was poured into ethanol. The collected precipitate was washed with excess ethanol and *n*-hexane. Recrystallization from toluene afforded 1,2-bis(4-methoxyphenyl)-3,4,5,6-tetraphenylbenzene as a pale brown solid (195 mg, 0.33 mmol; yield 46%).  $^1H$  NMR (300 MHz,  $CDCl_3$ ):  $\delta$  = 6.88–6.78 (m, 20H; Ph), 6.71 (d,  $J$  = 8.8 Hz, 4H; Ph  $\beta$  to -OMe), 6.41 (d,  $J$  = 8.8 Hz, 4H; Ph  $\alpha$  to -OMe), 3.61 ppm (s, 6H; Me).  $^{13}C$  NMR (75 MHz,  $CDCl_3$ ):  $\delta$  = 156.9, 140.9, 140.8, 140.6, 140.2, 133.2, 132.4, 131.4, 129.09, 126.6, 126.5, 125.05, 112.2, 54.9 ppm. ESI-TOF MS:  $m/z$ : calcd for  $C_{44}H_{34}O_2$ : 594.26; found: 617.3  $[M+Na]^+$ .

To a solution of 1,2-bis(4-methoxyphenyl)-3,4,5,6-tetraphenylbenzene (122 mg, 0.20 mmol) in dichloromethane (5 mL) was added dropwise boron tribromide (0.35 mmol) in dichloromethane (0.85 mL) at  $-40^\circ C$ . The mixture was stirred for an additional 18 h as the temperature increased to  $25^\circ C$ , followed by quenching by addition of water (5 mL). The target material was extracted with ethyl acetate and dried over anhydrous sodium sulfate. Colourless powder (113 mg, 0.20 mmol; 97%).  $^1H$  NMR (300 MHz,  $CDCl_3$ ):  $\delta$  = 7.00 (s, 2H; OH), 6.87–6.75 (m, 20 H; Ph), 6.63 (d,  $J$  = 8.5 Hz, 4H; Ph  $\beta$  to OH), 6.35 ppm (d,  $J$  = 8.5 Hz, 4H; Ph  $\alpha$  to OH).  $^{13}C$  NMR (75 MHz,  $CDCl_3$ ):  $\delta$  = 154.3, 141.3, 141.1, 140.8, 140.2, 132.6, 131.7, 126.71, 126.66, 125.2, 125.13, 114.0 ppm. ESI-TOF MS:  $m/z$ : calcd for  $C_{42}H_{30}O_2$ : 566.22; found: 566.2  $[M-H]^+$ .

#### 4.5. 1,2-Bis{4-[2,9(10),16(17)-tris(*tert*-butyl)subphthalocyaninatoboron(III)oxyphenyl]-3,4,5,6-tetraphenylbenzene, *bis*-[B(SubPc)] 2

A mixture of 1,2-bis(4-hydroxyphenyl)-3,4,5,6-pentaphenylbenzene (29 mg, 0.050 mmol) and Cl[B(SubPc)] (85 mg, 0.14 mmol) was refluxed in dry toluene (4 mL) and ethyl acetate (0.5 mL) for 88 h. After removal of the solvent under reduced pressure, the residue was dissolved in chloroform (20 mL) and successively washed with saturated aqueous sodium hydrogencarbonate (20 mL) and brine (20 mL). The organic layer was dried over anhydrous sodium sulfate. The residue was purified by silica-gel column chromatography with hexane/ethyl acetate (5/1, v/v) as the eluent, followed by passing through a Sephadex column with ethyl acetate as the eluent. Purple solid (47 mg, 0.028 mmol; 55% based on 1,2-bis(4-hydroxyphenyl)-3,4,5,6-pentaphenylbenzene).  $^1H$  NMR (300 MHz,  $CDCl_3$ ):  $\delta$  = 8.83, 8.76 (s, s, 6H; SubPc- $\alpha_{(1)}$ ), 8.67, 8.60 (d, d,  $J$  = 8.4 Hz, 6H; SubPc- $\alpha_{(4)}$ ), 7.94–7.89 (brm, 6H; SubPc- $\beta$ ), 6.79–6.56 (m, 16H; Ph), 6.48 (d,  $J$  = 7.2 Hz, 4H; 3,6-Ph  $\alpha$  to central Ph), 5.91 (d, 4H,  $J$  = 8.4 Hz, Ph  $\beta$  to O-B(SubPc)), 5.02–4.72 (m, 4H; Ph  $\alpha$  to O-B(SubPc)), 1.54, 1.52, 1.51 (s, s, s, 54H; *t*Bu).  $^{13}C$  NMR (126 MHz,  $CDCl_3$ ):  $\delta$  = 153.60, 153.59, 153.55, 153.53, 151.30, 151.24, 151.10, 151.01, 150.97, 150.84, 149.86, 149.82, 140.9, 140.5, 140.1, 139.95, 139.91, 133.6, 131.75, 131.69, 131.5, 131.33, 131.25, 131.19, 131.13, 128.75, 128.71,

128.70, 128.66, 127.7, 126.41, 126.36, 124.9, 124.75, 121.7, 118.26, 118.20, 118.06, 117.9, 117.8, 117.6, 35.8, 31.7 ppm.  $^{11}B$  NMR (96 MHz,  $CDCl_3$ ):  $\delta$  =  $-14.9$  ppm (brs). MALDI-TOF MS:  $m/z$  calcd for  $C_{114}H_{100}B_2N_{12}O_2$  1690.83; found 1690.02  $[M]^+$ . UV-vis (toluene):  $\lambda_{\max}$  = 566 nm (Q band).

#### 4.6. 1-{4-[2,9(10),16(17)-Tris(*tert*-butyl)subphthalocyaninatoboron(III)oxyphenyl]-2,3,4,5,6-pentaphenylbenzene, *mono*-[B(SubPc)] 3

A mixture of 1-(4-hydroxyphenyl)-2,3,4,5,6-pentaphenylbenzene<sup>19</sup> (75 mg, 0.14 mmol) and Cl[B(SubPc)] (26 mg, 0.043 mmol) was refluxed in dry toluene/1,4-dioxane (4 mL/2 mL) for 34 h. The residue was purified by silica-gel chromatography with *n*-hexane/ethyl acetate (5/1, v/v) as the eluent, followed by a second silica-gel column with the gradient solvent system of toluene/ethyl acetate (100/0 to 55/1, v/v). The desired product was eluted from a Sephadex column with ethyl acetate as a purple solid (7.8 mg, 7  $\mu$ mol; 16% based on Cl[B(SubPc)]).  $^1H$  NMR (300 MHz,  $CDCl_3$ ):  $\delta$  = 8.86, 8.83 (s, s, 3H; SubPc- $\alpha_{(1)}$ ), 8.76, 8.73 (d, d,  $J$  = 8.4 Hz, 3H; SubPc- $\alpha_{(4)}$ ), 7.95 (d, 3H,  $J$  = 8.4 Hz, SubPc- $\beta$ ), 6.82–6.60 (m, 21H, Ph), 6.57 (d, 4H,  $J$  = 6.7 Hz, 2,6-Ph  $\alpha$  to central Ph), 6.12 (d,  $J$  = 8.5 Hz, 2H; Ph  $\beta$  to O-B(SubPc)), 4.91 (d,  $J$  = 8.5 Hz, 2H; Ph  $\alpha$  to O-B(SubPc)), 1.57–1.55 ppm (m, 27H; *t*Bu).  $^{13}C$  NMR (75 MHz,  $CDCl_3$ ):  $\delta$  = 153.7, 140.7, 140.33, 140.25, 139.9, 131.8, 131.4, 131.2, 127.8, 126.5, 125.0, 124.9, 121.6, 118.6, 117.5, 35.8, 31.7 ppm.  $^{11}B$  NMR (96 MHz,  $CDCl_3$ ):  $\delta$  =  $-15.0$  ppm (brs). MALDI-TOF MS:  $m/z$  calcd for  $C_{78}H_{65}BN_6O$  1112.53; found 1112.53  $[M]^+$ . UV-vis (toluene):  $\lambda_{\max}$  = 566 nm (Q band).

#### 4.7. [2,9(10),16(17)-tris(*tert*-butyl)subphthalocyaninatoboron(III)oxy]benzene, PhO[B(SubPc)] 4

A mixture of Cl[B(SubPc)] (21 mg, 0.035 mmol) and phenol (19 mg, 0.2 mmol) was refluxed in dry toluene (3 mL) in the dark for 3.5 h. After removal of the solvent, the residue was redissolved in chloroform (20 mL) and successively washed with saturated aqueous sodium hydrogencarbonate (20 mL) and brine (20 mL). The organic layer was dried over anhydrous sodium sulfate. The titled material was eluted from a silica-gel column chromatography with *n*-hexane/ethyl acetate (8/1, v/v) as the eluent. PhO[B(SubPc)] 4 was obtained as purple solid (22 mg, 0.033 mmol; 95% based on Cl[B(SubPc)]).  $^1H$  NMR (300 MHz,  $CDCl_3$ ):  $\delta$  = 8.88, 8.85 (s, s, 3H; SubPc- $\alpha_{(1)}$ ), 8.77, 8.75 (d, d,  $J$  = 8.4 Hz, 3H; SubPc- $\alpha_{(4)}$ ), 7.97 (d,  $J$  = 8.4 Hz, 3H; SubPc- $\beta$ ), 6.75 (dd,  $J$  = 8.4, 7.4 Hz, 2H; Ph  $\beta$  to O-B(SubPc)), 6.60 (t,  $J$  = 8.4 Hz, 1H; *p*-Ph), 5.39 (d,  $J$  = 7.4 Hz, 2H; Ph  $\alpha$  to O-B(SubPc)), 1.55, 1.54 ppm (s, s, 27H; *t*Bu).  $^{11}B$  NMR (96 MHz,  $CDCl_3$ ):  $\delta$  =  $-14.8$  ppm (brs). MALDI-TOF MS:  $m/z$ : calcd for  $C_{42}H_{41}BN_6O$ : 656.34; found: 656.36  $[M]^+$ . UV-vis (toluene):  $\lambda_{\max}$  = 567 nm (Q band).

#### 4.8 Analytical methods of steady-state fluorescence/excitation anisotropy measurement

Fast energy migration redistributes the polarization at the excited state, where it is expected to be reduced the ratio of fluorescence anisotropy ( $r$ ). Then, steady-state fluorescence anisotropy was observed in polyethylene glycol (PEG;  $M_w$  = ca. 200) as viscous medium to minimize molecular reorientation.<sup>3</sup> A comparison is available to evaluate the qualitative energy migration.

The fluorescence anisotropy ratio,  $r$ , employing vertically polarized excitation light was compared at each wavelength based on the following equation:<sup>3</sup>

$$r = [I_{//} - gI_{\perp}] / [I_{//} + 2gI_{\perp}]$$

where  $g$  is the correction factor to calibrate the experimental error arising from instrumental set-up at each wavelength. The similar experiments employing horizontally polarized incident light gave the  $g$  value defined as the equation;  $g = I'_{\perp} / I'_{//}$ .

## Acknowledgements

This work was financially supported through a Grant-in-Aid for Young Scientists (B) (No. 21750123) from JSPS (Japan Society of the Promotion of Science), and also the Kyoto-Advanced Nanotechnology Network program with a technical assistance by Ms. Yoshiko Nishikawa (Nara Institute of Science and Technology). The authors thank Dr Sadahiro Masuo and Prof. Akira Itaya (Department of Macromolecular Science and Engineering, Kyoto Institute of Technology) for time-resolved fluorescence measurements, and Dr Johannes K. Sprafke and Dr Hazel A. Collins (Chemistry Research Laboratory, University of Oxford) for a HyperChem simulation and correcting the entire text in the original draft.

## References

- (a) G. McDermott, S. M. Prince, A. A. Freer, A. M. Hawthornthwaite-Lawless, M. Z. Papiz, R. J. Cogdell and N. W. Isaacs, *Nature*, 1995, **374**, 517–521; (b) A. W. Roszak, T. D. Howard, J. Souhall, A. T. Gardiner, C. J. Law, N. W. Isaacs and R. J. Cogdell, *Science*, 2003, **302**, 1969–1972.
- (a) Y. Nakamura, N. Aratani and A. Osuka, *Chem. Soc. Rev.*, 2007, **36**, 831–845; (b) Y. Kuramochi, A. S. D. Sandanayaka, A. Satake, Y. Araki, K. Ogawa, O. Ito and Y. Kobuke, *Chem.–Eur. J.*, 2009, **15**, 2317–2327.
- (a) H. S. Cho, H. Rhee, J. K. Song, C.-K. Min, M. Takase, N. Aratani, S. Cho, A. Osuka, T. Joo and D. Kim, *J. Am. Chem. Soc.*, 2003, **125**, 5849–5860; (b) A. Morandeira, E. Vauthey, A. Schuwey and A. Gossauer, *J. Phys. Chem. A*, 2004, **108**, 5741–5751.
- (a) S. Rucareanu, A. Schuwey and A. Gossauer, *J. Am. Chem. Soc.*, 2006, **128**, 3396–3413; (b) M. Hoffman, J. Kärrbratt, M.-H. Chang, L. M. Herz, B. Albinsson and H. L. Anderson, *Angew. Chem., Int. Ed.*, 2008, **47**, 4993–4996; (c) M. C. O'Sullivan, J. K. Sprafke, D. V. Kondratuk, C. Rinfray, T. D. W. Claridge, A. Saywell, M. O. Blunt, J. N. O'Shea, P. H. Beton, M. Malfois and H. L. Anderson, *Nature*, 2011, **469**, 72–75.
- G. Bottari and T. Torres, *Chem. Commun.*, 2004, 2668–2669.
- (a) D. Gust, *J. Am. Chem. Soc.*, 1977, **99**, 6980–6982; (b) D. Gust and A. Patton, *J. Am. Chem. Soc.*, 1978, **100**, 8175–8181; (c) A. Patton, J. W. Dirks and D. Gust, *J. Org. Chem.*, 1979, **44**, 4749–4752; (d) D. Gust and M. W. Fagan, *J. Org. Chem.*, 1980, **45**, 2511–2512; (e) H. Pepermans, R. Willem, M. Gielen and C. Hoogzand, *J. Org. Chem.*, 1986, **51**, 301–306.
- (a) C. G. Claessens, D. González-Rodríguez and T. Torres, *Chem. Rev.*, 2002, **102**, 835–853; (b) N. Kobayashi, T. Ishizaki, K. Ishii and H. Konami, *J. Am. Chem. Soc.*, 1999, **121**, 9096–9110.
- (a) C. G. Claessens, D. González-Rodríguez, D. del Rey, T. Torres, G. Mark, H.-P. Schuchmann, C. von Sonntag, J. G. MacDonald and R. S. Nohr, *Eur. J. Org. Chem.*, 2003, 2547–2551; (b) Very recently, more advanced method has been reported in the reference 10c.
- (a) D. González-Rodríguez, T. Torres, D. M. Guldi, J. Rivera, M. Á. Herranz and L. Echegoyen, *J. Am. Chem. Soc.*, 2004, **126**, 6301–6313; (b) D. González-Rodríguez, T. Torres, M. M. Olmstead, J. Rivera, M. Á. Herranz, L. Echegoyen, C. A. Castellanos and D. M. Guldi, *J. Am. Chem. Soc.*, 2006, **128**, 10680–10681; (c) D. González-Rodríguez, T. Torres, M. Á. Herranz, L. Echegoyen, E. Caronell and D. M. Guldi, *Chem.–Eur. J.*, 2008, **14**, 7670–7679.
- (a) T. Fukuda, M. M. Olmstead, W. S. Durfee and N. Kobayashi, *Chem. Commun.*, 2003, 1256–1257; (b) G. E. Morse, A. S. Paton, A. Lough and T. P. Bender, *Dalton Trans.*, 2010, **39**, 3915–3922; (c) J. Guilleme, D. González-Rodríguez and T. Torres, *Angew. Chem., Int. Ed.*, 2011, **50**, 3506–3509.
- See the Supporting Information.
- (a) I. Tinoco Jr., *J. Am. Chem. Soc.*, 1960, **82**, 4785–4790; (b) M. Kasha, M. A. El-Bayoumi and W. Rhodes, *J. Chim. Phys.*, 1961, **58**, 916–925.
- (a) N. Mataga, Y. Kaifu and M. Koizumi, *Bull. Chem. Soc. Jpn.*, 1955, **28**, 690–691; (b) N. Mataga, Y. Kaifu and M. Koizumi, *Bull. Chem. Soc. Jpn.*, 1956, **29**, 373–379.
- (a) T. Hayashi, T. Suzuki, N. Mataga, Y. Sakata and S. Misumi, *J. Phys. Chem.*, 1977, **81**, 420–423; (b) F. C. De Shryver, P. Collart, J. Vandendriessche, R. Goedeweck, A. Swinnen and M. V. der Auweraer, *Acc. Chem. Res.*, 1987, **20**, 159–166.
- Fluorescence quantum yield ( $\Phi_F$ ) was determined based on the value for Cl[B(SubPc)] in benzene ( $\Phi_F = 0.16$ ) as reported in B. del Rey, U. Keller, T. Torres, G. Rojo, F. Agulló-López, S. Nonell, C. Martí, S. Brasselet, I. Ledoux and J. Zyss, *J. Am. Chem. Soc.*, 1998, **120**, 12808–12817.
- Anthracenes: (a) H. Yao, T. Okada and N. Mataga, *J. Phys. Chem.*, 1989, **93**, 7388–7394; (b) M. Schütz and R. Schmidt, *J. Phys. Chem.*, 1996, **100**, 2012–2018; (c) K. Nishiyama, T. Honda, H. Reis, U. Müller, K. Müllen, W. Baumann and T. Okada, *J. Phys. Chem. B*, 1998, **102**, 2934–2943; (d) J. J. Piet, W. Schuddeboom, B. R. Wegewijs, F. C. Grozema and J. M. Warman, *J. Am. Chem. Soc.*, 2001, **123**, 5337–5347 and cited therein.
- Naphthalene bisimide: N. Banerji, A. Fürstenberg, S. Bhosale, A. Sission, N. Sakai, S. Matile and E. Vauthey, *J. Phys. Chem. B*, 2008, **112**, 8912–8922.
- Perylene and perylene bisimide (a) J. M. Giaimo, A. V. Gusev and M. R. Wasielewski, *J. Am. Chem. Soc.*, 2002, **124**, 8530–8531; (b) V. Markovic, D. Villamaina, I. Barbanov, L. M. L. Daku and E. Vauthey, *Angew. Chem., Int. Ed.*, 2011, **50**, 7596–7598, and cited therein.
- S. Matsumura, A. R. Hlil, C. Lepiller, J. Gaudet, D. Guay and A. S. Hay, *Macromolecules*, 2008, **41**, 277–280.
- K. Kobayashi, T. Shirasaka, A. Sato, E. Horn and N. Furukawa, *Angew. Chem., Int. Ed.*, 1999, **38**, 3483–3486.